



Trade Science Inc.

ISSN : 0974 - 7486

Volume 7 Issue 5

Materials Science

An Indian Journal

Full Paper

MSAIJ, 7(5), 2011 [302-309]

Microstructure and mechanical properties of aged nickel base superalloy

Nader El-Bagoury^{1,2}

¹Materials and Corrosion Group, Chemistry Department, Faculty of Science, TAIU University, P.O. Box 888, El-Haweyah, El-Taif, (SAUDIARABIA)

²Casting Technology Lab., Manufacturing Technology Dept., Central Metallurgical Research and Development Institute, CMRDI, P. O. Box 87 Helwan, Cairo, (EGYPT)

E-mail: nader_elbagoury@yahoo.com

Received: 23rd February, 2011 ; Accepted: 5th March, 2011

ABSTRACT

The effect of aging process at 845° C for 24 h and casting conditions on the microstructure and mechanical properties of Ni base superalloys were investigated. Alloys under investigation were manufactured by investment casting under various conditions of cooling rate and superheat. These alloys were solution treated at 1120 and 1180° C followed by air cooling before aging process. The volume fraction of TCP phases decreases with increasing casting superheat and lowering cooling rate. The grain size of aged specimens and solution treated at 1180° C is coarser than ones solution treated at 1120° C. The V_f of γ' particles in case of aged with low superheat specimen is higher than that in high superheat one after solution at 1120 and 1180° C. The V_f of γ' in case of aged and solution treated at 1120° C is higher than that aged with solution treated at 1180° C. Hardness measurements of aged alloys with low and high superheat specimens solution treated at 1120° C are higher than that of 1180° C. © 2011 Trade Science Inc. - INDIA

KEYWORDS

Ni base superalloy;
Aging;
Microstructure;
 η , σ and γ' phases;
DSC;
Mechanical properties.

INTRODUCTION

Nickel base superalloys used for modern gas turbines are continually being developed to increase thrust, operating efficiency and durability. For many years, Ni base superalloys such as IN738LC and GTD 111 alloys have been used in gas turbines as blades at high temperature because of its excellent high temperature mechanical properties^[1-5]. Generally, the Ni-base superalloys with complex and multi-phase microstructures are stable at high temperatures and this characteristic is

the main reason for using them in critical and severe service conditions^[7-9].

The strengthening of nickel-based superalloys is mainly obtained by the coherent precipitation of a large amount of Ni₃Al type γ' % phase in a nickel-based γ matrix. The morphology of the γ' % precipitates in these alloys has been well documented and a large variety of the γ' % precipitate shapes has been observed (spheres, cubes, aligned cubes, plates, short plates, doublet of short plates, octet of cubes, large plates, rafts, . . .)^[10-13].

Topologically closed-packed (TCP) phases are

intermetallic compounds that occur in a plate-like morphology, which of course, appears as needles or single-plane microstructure. These intermetallic compounds form when the ratio of refractory metals and chromium to cobalt + nickel in the alloy matrix exceeds certain levels, as defined by the phase relations for the systems involved^[14].

The heat treatments usually recommended for nickel-base superalloys are suggested primarily to produce high volume fraction and better size distribution of γ' precipitates which give optimum stress rupture property. In as-cast alloys with a high volume fraction of γ/γ' eutectic, the complete dissolution of γ' by the appropriate heat treatment is of extreme importance^[15]. The high melting temperature of Ni base superalloys frequently allows for refinement of the γ' microstructure with a solution heat treatment followed by one or more steps of ageing heat treatments. Both γ' precipitate size and volume fraction (V_f) can significantly influence the mechanical properties of the single crystal nickel-base superalloys at room and elevated temperature^[16].

In this study, the effect of aging heat treatment process on microstructure and mechanical properties of an experimental Ni base superalloy will be investigated. TCP phases and γ' particle morphology, size and volume fraction will be evaluated under casting conditions of cooling rate and superheat levels.

EXPERIMENTAL PROCEDURES

The chemical composition of the investigated Ni base superalloys in this study is shown in Figure 1. These alloys were melted under vacuum atmosphere before casting under various casting conditions of cooling rates and superheat levels. Low (L) and high (H) superheat levels were applied into two castings. Each alloy, H and L alloys, accompanied by three cooling rates; fast, medium and slow.

These Ni base superalloys were solution treated at different conditions of 1120 and 1180 °C for 2 h followed by air cooling. Further aging heat treatment at 845 °C for 24 h was accomplished for both solution treated alloys.

Optical emission apparatus, ARL3560OES as well as Ni base software were used to determine the chemical composition of the heat treated alloys.

Characterization for microstructure studies including morphology and volume fraction of different phases was carried out by both Zeiss light optical microscope fitted with Hitachi digital camera and JOEL JSM-5410 Scanning Electron Microscope (SEM). The specimens for microstructure examination were ground and polished according to ASTM standard E3 and E768, then etched with 50 ml HCl + 2 ml H₂O₂ (30%) solution. The study of the microanalysis and segregation for alloying elements was performed using EDS in JEOL JSM5410.

Differential scanning calorimetry (DSC) analysis was performed using a Netzch STA 449 F3 Jupiter instrument to examine the crystallization behavior of the alloy. All samples were heated at a constant rate of 10°C/min and duplicate samples were evaluated for each condition.

The Vickers hardness was measured with Akashi Hardness Tester Machine (Akashi Co. Ltd.) under a load of 60 Kg. The mean value over ten measurements was evaluated.

TABLE 1 : Chemical composition of experimental Ni base superalloy, mass %.

Elements Alloy	C	Cr	Mo	W	Ti	Co	Al	Nb	Ta	Ni
As cast (H)	0.54	16.95	2.45	4.36	5.88	10.48	1.49	0.10	1.86	Bal.
As cast (L)	0.47	16.97	2.39	4.27	5.74	10.37	1.41	0.12	1.93	Bal.

RESULTS AND DISCUSSION

As cast structure of Ni base superalloys

The microstructure of the as cast experimental Ni base superalloys used in the present work, consists of primary γ , interdendritic γ/γ' , MC carbides and TCP phases such as η and σ phases in the interdendritic zones, as shown in Figure 1.

The highest V_f of interdendritic γ/γ' found with highest cooling rate and lowest melt superheat. Whereas the V_f of σ and η phases increases as the melt superheat increases and the cooling rate decreases^[17].

Bimodal, spheroidal and cuboidal shape, and duplex precipitates, fine and coarse γ' phase are found in the as cast microstructure.

In dendritic region, there are fine γ' precipitates while in interdendritic region, coarse size γ' precipitates exist, as it has been also observed by Kim et al.^[18].

Full Paper

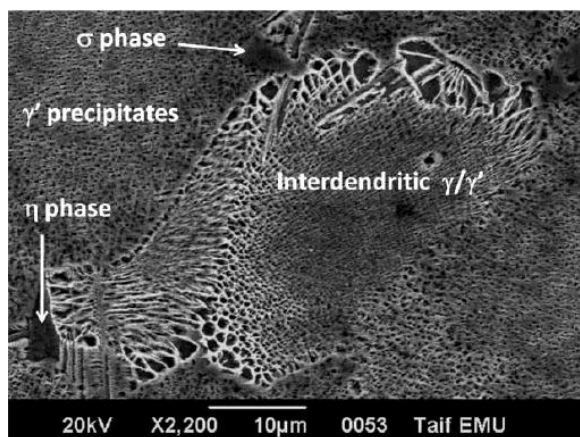


Figure 1 : Microstructure of as cast Ni base superalloy^[17].

TABLE 2 give the micro-chemical analysis of TCP phases like η and σ phases. η phase has high levels of Ti and Ni elements whereas Cr, Mo and W are the main elements in which σ phase composed of^[17].

TABLE 2 : EDS chemical analysis of σ and η phase in aged alloys^[17].

Elements Phase	C	Cr	Mo	W	Ti	Co	Al	Nb	Ta	Ni
η	0.19	4.31	0.84	1.17	15.94	7.19	1.53	0.34	3.00	Bal.
σ	0.78	36.75	20.37	10.01	2.29	9.68	0.47	--	3.45	Bal.

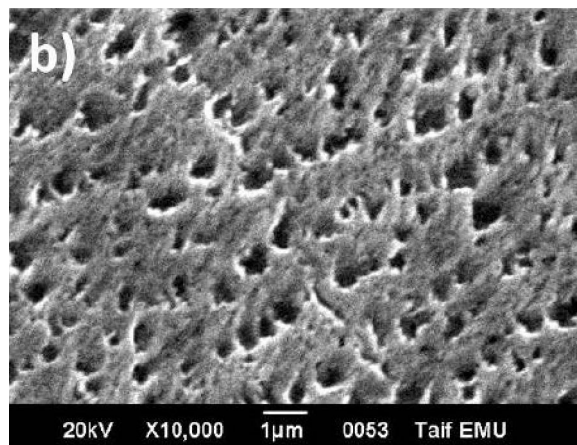
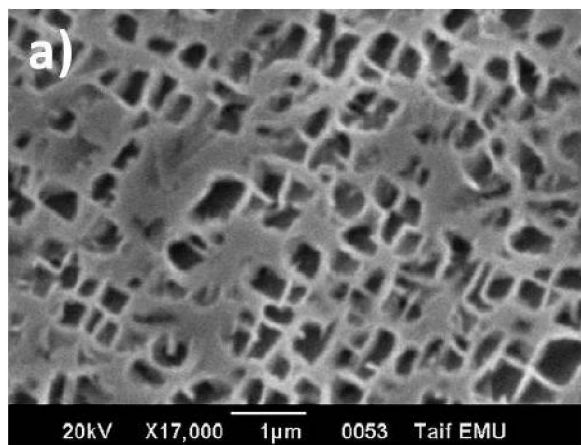


Figure 2 : γ' in as cast (a) and heat treated microstructures at 1120 °C^[19].

The effect of solution treatment temperature on the V_f of η phase for different specimens is given in TABLE

TABLE 3 : Effect of solution temperature on V_f of η phase^[19].

Specimen	V_f at solution treatment Temperature (%)	
	at 1120 °C	at 1180 °C
L1	2.76	1.23
H1	4.64	2.36
L3	1.27	0.45
H3	3.25	1.89

Solution treated microstructure

Solution treatment was carried out for 2h at both 1120 and 1180°C followed by air cooling. The solution treatment at 1120°C represents the standard solution treatment while that at 1180°C represents the modified solution treatment. DSC measurements, SEM and EDS emphasized that the σ nodular and interdendritic γ/γ' phases found in as cast structure were entirely vanish after solution treatment either at 1120 or 1180° C^[19].

After solution treatment with various conditions for all as cast specimens, the interdendritic γ/γ' phase vanished completely from these microstructures.

Density or V_f as well as morphology and size of γ' precipitates is affected by the solution treatment conditions. The morphology of as cast coarse cuboidal γ' precipitates changes to fine spheroidal ones after solution treatment processes, as shown in Figure 2. The V_f of these precipitates in as cast microstructure decreases by solution treatment. Solution treatment with 1120°C has higher V_f of γ' precipitates than solution treatment after 1180°C. Coarse γ' particles first coalesce with each other then dissolved in the matrix with solution treatment.

3. Elevating the solution treatment temperature from 1120 to 1180°C, affect significantly the V_f of η phase. This V_f decreases by increasing solution temperature from 1120 to 1180 °C for the same specimen.

Influence of aging on microstructure

Figures 3 and 4 show the aged microstructures at 845° C of L and H specimens after solution treatment at 1120 and 1180° C, respectively. The aged microstructures of L and H specimens with various cooling

rates, L1, L3, H1 and H3 are shown in Figures 3 and 4. General speaking, the V_f of TCP phases in interdendritic regions of 1120° C specimens is higher than that of 1180° C for both L and H alloys. In other words, high solution temperature dissolves TCP phases such as σ and η phases in the γ matrix.

Moreover, casting superheat level has a great effect on the V_f of TCP phases. Superheat level has inverse relationship with TCP V_f , where decreasing superheat level increases the of TCP phases in interdendritic regions, as it can be seen in Figures 3 and 4.

Additionally, needle-like η phase can be noticed in the microstructure of 1120° C after aging at 845° C, as shown in Figure 3. However, this morphology of η phase entirely vanished from the microstructure of 1180° C, as shown in Figure 4.

The grain size of aged alloys affected as well by the solution temperature^[17]. It can be easily recognized that the grain size of all L and H alloys with 1180° C is coarser than that of 1120° C for the same conditions of L and H specimens, as shown in Figure 3 and 4.

Two types of carbides are observed in the microstructure of H and L specimens after aging at 845° C for 24 h; primary MC and $M_{23}C_6$ carbides. MC carbides have an irregular blocky morphology at grain boundaries and in interdendritic zones. However, $M_{23}C_6$ carbides are located at the border between η and γ phases.

According to chemical analysis of carbides given in TABLE 2, the major alloying elements in MC carbides are Ta and Ti in addition to carbon. Additionally, the $M_{23}C_6$ carbides consist mainly of Cr and W beside carbon.

Blocky MC carbides are smaller in size in L specimen in comparison with H specimen after aging at 845° C for 24 h. Moreover, $M_{23}C_6$ carbides observed in L specimen are small separated particles at the grain boundaries. While in H specimen, these small separated $M_{23}C_6$ particles grow and congregate into a wide continuous carbide chain at grain boundaries.

Figures 6 and 7 show the γ' precipitates in both aged L and H specimens after solution at 1120 and 1180° C, respectively.

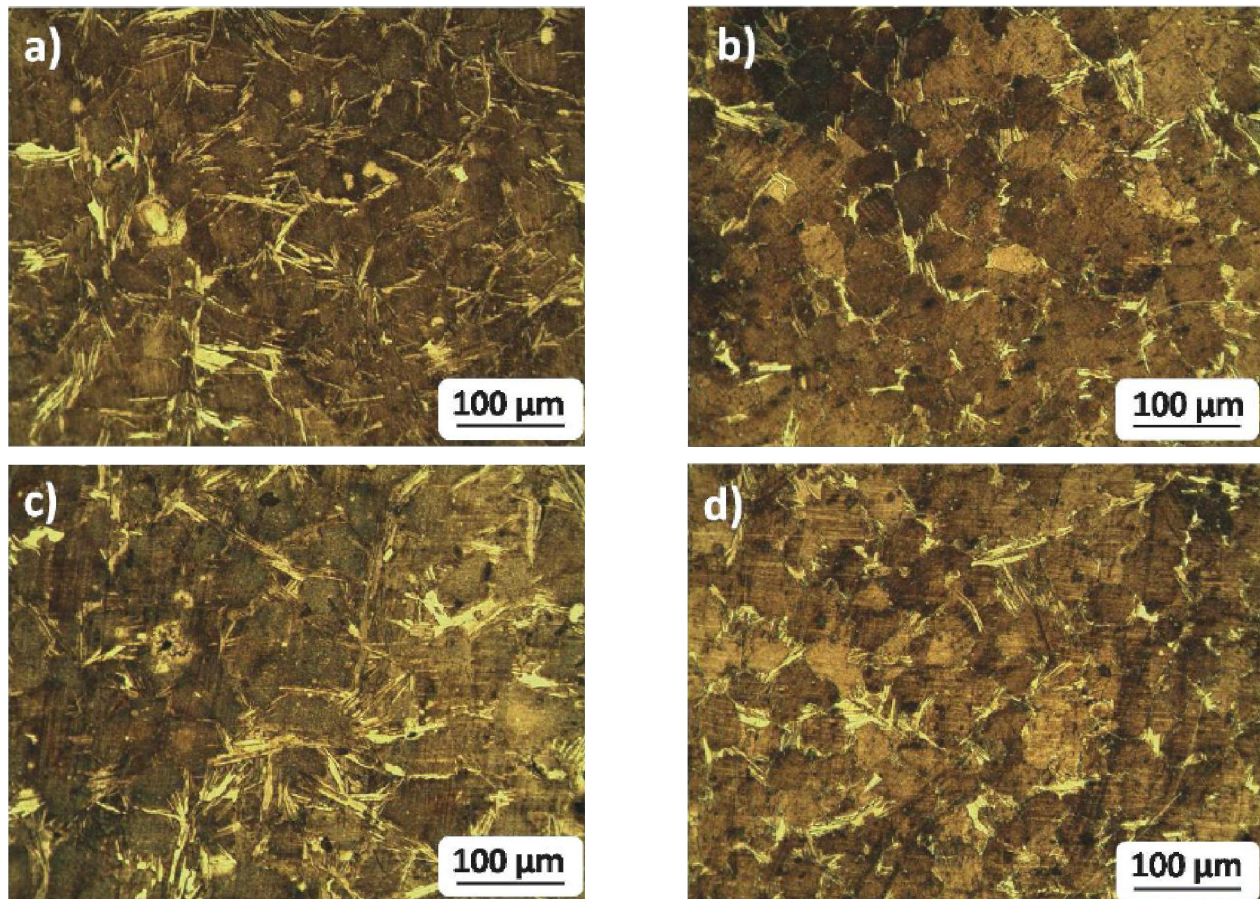


Figure 3 : Aged microstructure at 845°C after solution treated at 1120°C of; H1, b) L1, c) H3 and d) L3 alloys.

Full Paper

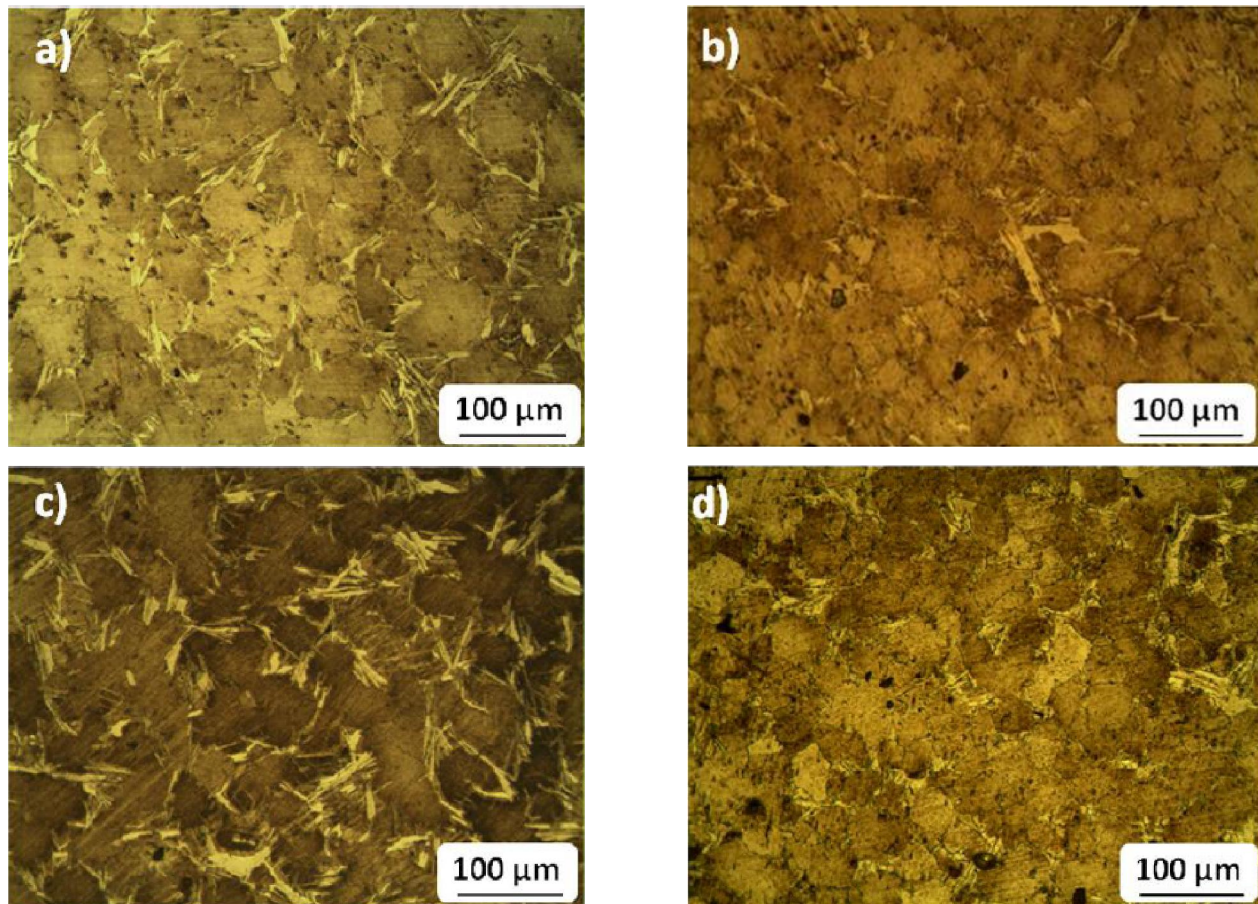


Figure 4 : Aged microstructure at 845°C after solution treated at 1180°C of; H1, b) L1, c) H3 and d) L3 alloys.

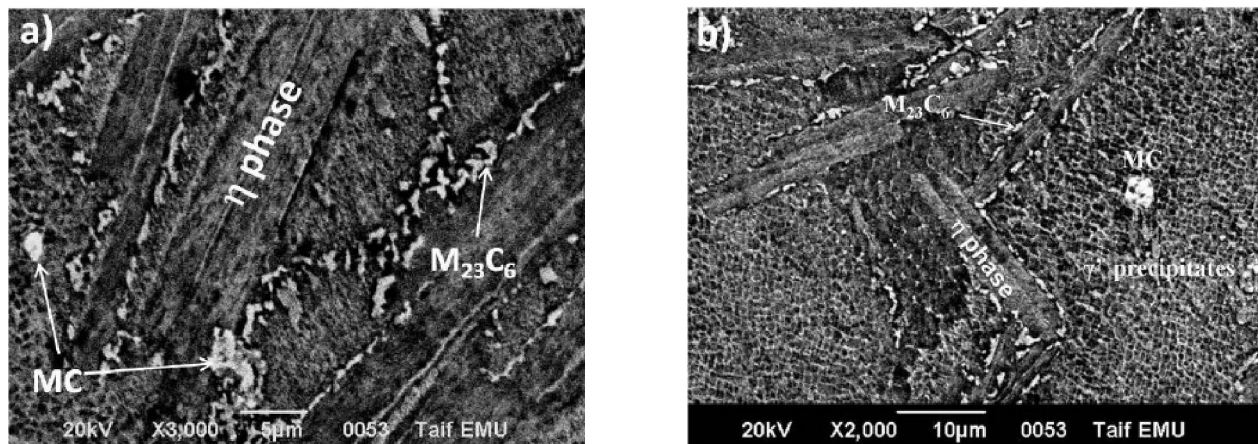


Figure 5 : Aged microstructure at 845°C of a) H1 and b) L1 solution treated at 1180°C.

TABLE 4 : EDS chemical analysis of carbides in aged alloys.

Elements Phase	C	Al	Ti	Cr	Co	Ni	Nb	Mo	Ta	W
MC	8.35	0.23	24.07	2.03	1.08	5.06	0.24	1.02	55.38	2.54
M ₂₃ C ₆	11.23	0.70	2.30	64.4	1.86	5.64	0.38	1.74	2.55	9.2

The size of γ' particles in aged H specimen at 845°C for 24 h is larger than that in L specimen in both cases of solution treatment, 1120 and 1180°C, as shown

in Figures 6 and 7^[20].

The V_f of γ' particles in case of aged L specimen is higher than that in H one after solution at 1120 and 1180°C, as shown in Figures 6 and 7.

Increasing the solution temperature from 1120 to 1180°C decreasing the V_f of γ' particles in both L and H specimens. Whereas the solution temperature elevated the coarse γ' precipitates dissolved in the matrix

lowering the V_f of γ' particles^[20].

A the morphology of γ' particle is only round with

different sizes in the L and H specimens with 1120 and 1180° C as shown in Figures 6 and 7.

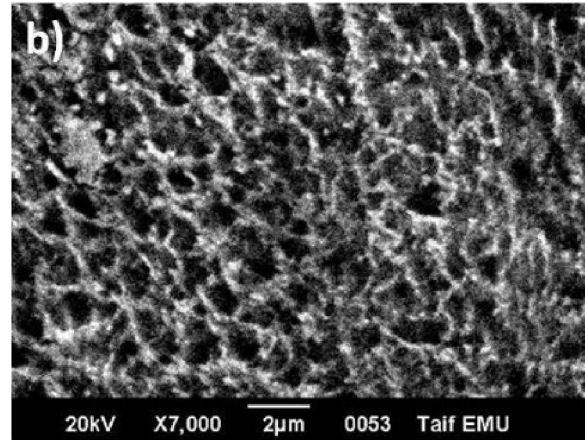
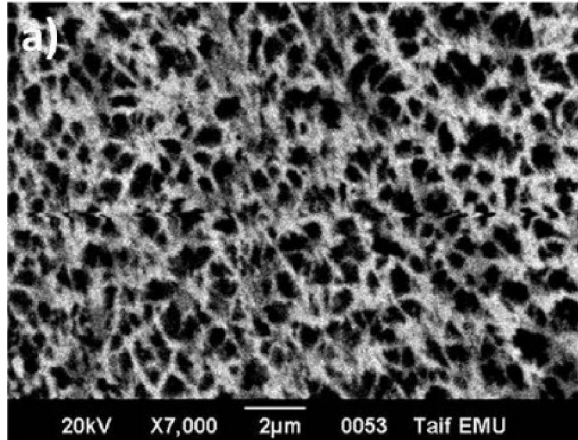


Figure 6 : γ' precipitates in aged microstructure at 845° C of H specimen with solution temperature at 1120° C a) L1 and b) H1 after aging at 845 °C.

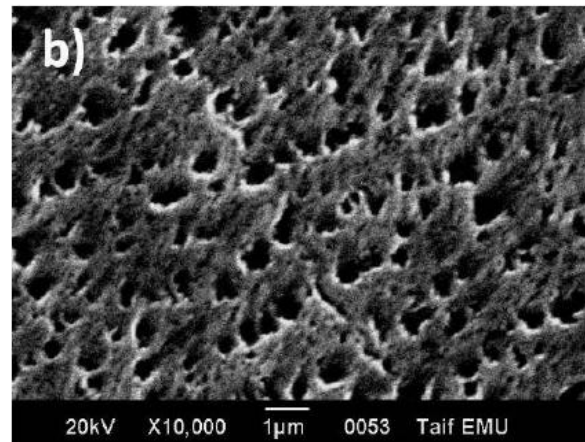
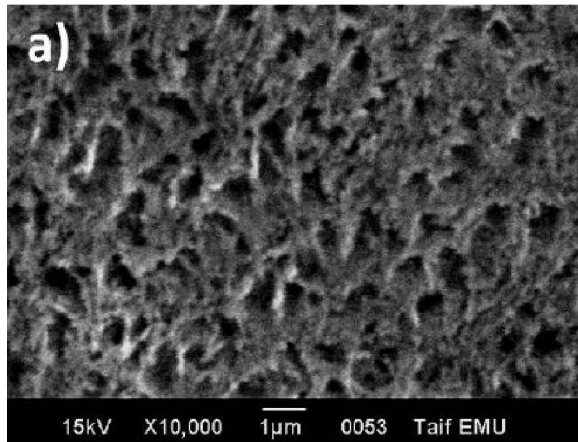


Figure 7 : γ' precipitates in aged microstructure at 845° C of H specimen with solution temperature at 1180° C a) L1 and b) H1 after aging at 845 °C.

Hardness measurements

TABLE 5 : Hardness values of aged specimens at 1120 and 1180° C

Alloy	L1	L2	L3	H1	H2	H3
1120°C	472	467	445	462	454	440
1180°C	450	438	427	446	436	425

Hardness measurements for aged specimens at 845 C for 24 h and solution treated at 1120 and 1180° C were evaluated. Hardness value has a strong relationship with the γ' characteristics especially volume fraction and size. Moreover, cooling rate and superheat levels affect the hardness values as well. Hardness measurements of aged L and H specimens after solution at 1120 and 1180° C are given in TABLE 4. Highest values for hardness property obtained with

highest cooling rate specimens L1 and H1^[21]. Additionally, lowest hardness measurements achieved with lowest cooling rate specimens such as L3 and H3, as shown in Figure 8. Therefore, it could be concluded that hardness measurements increased with increasing cooling rate and vice versa. However, L specimens have higher hardness values than H specimens in both cases; 1120 and 1180° C, as shown in Figure 8. In other words, as the superheat level increases the hardness value decreased^[22].

Hardness measurements for L and H specimens with 1120° C are higher than that of 1180° C, as shown in Figure 8 (a) and (b). Moreover, the difference in hardness values between L and H specimens in case of 1120° C is wider than in 1180° C one, as shown in Figure 8 (a) and (b).

Full Paper

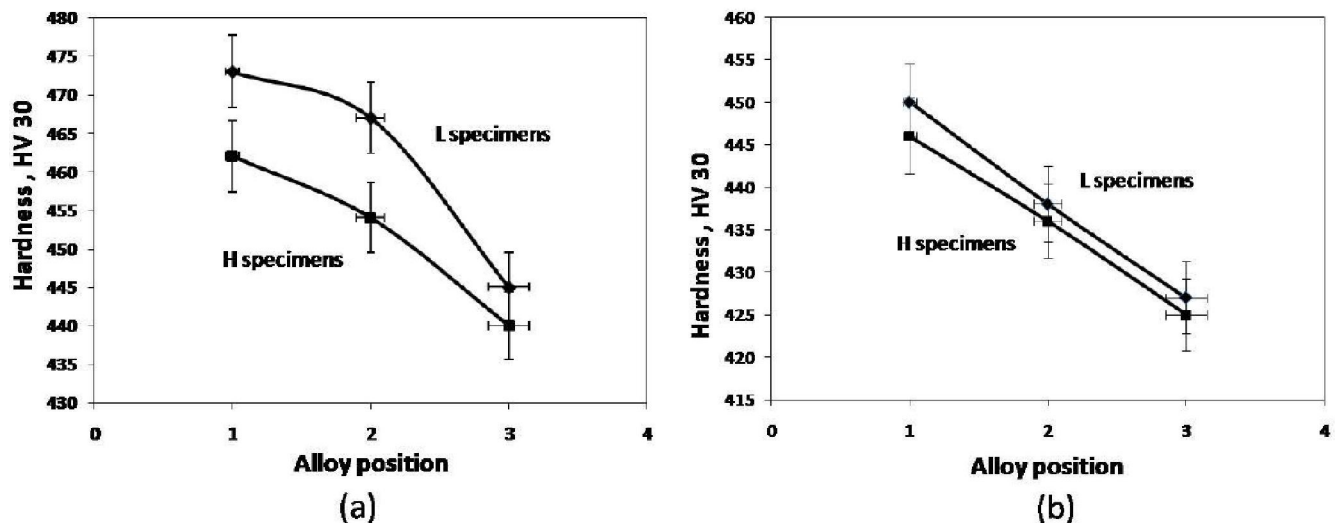


Figure 8 : Hardness measurements for L and H specimens after aging at (a) 1120 and (b) 1180° C.

As the cooling rate increases and superheat decreases the hardness value increased^[23,24]. This may be related to the smaller size of γ' in comparison with the conditions of lower cooling rate and higher superheat level, as shown in Figures 6 and 7.

Higher temperature of aging treatment, 1180° C, has higher effects on the dissolution of coarse γ' in the matrix than in case of 1120° C. Therefore the V_f of γ' in case of 1120° C is higher than that in 1180° C, which in turn increase the hardness values of 1120° C specimens than 1180° C ones. In the same direction, the size of γ' particles in 1120° C specimens is larger than that in case of 1180° C as shown in Figures 6 and 7. The variation of hardness values between L and H specimens are different because of the effectiveness of aging with solution at higher temperature, 1180° C, that diminish the V_f and size of γ' than in case of aging with solution at lower temperature, 1120° C. From the latter it can be concluded that in case of aging with solution at 1180° C specimens, the rate determining step is the aging temperature. However in aging with solution at 1120° C specimens, cooling rate and superheat level have a great influence on the hardness measurements in addition to the solution temperature level.

CONCLUSIONS

The results of aging at 845° C for 24 h on the microstructure and mechanical properties of Ni base superalloys that solution treated at 1120 and 1180 were

as follows:

1. The V_f of TCP phases in aged L and H specimens solution treated at 1120° C is higher than that of 1180° C.
2. The grain size of aged L and H specimens with 1180° C is larger than the grain size of solution treated at 1120° C.
3. The V_f of γ' particles in case of aged L specimen is higher than that in H one after solution at both 1120 and 1180° C.
4. The V_f of γ' precipitates in case of aged alloys solution treated at 1120° C is higher than that solution treated with 1180° C.
5. Hardness measurements of aged L and H specimens with 1120° C are higher than that of 1180° C.

REFERENCES

- [1] J.S.Houa, J.T.Guoa, L.Z.Zhoua, C.Yuana, H.Q.Ye; Materials Science and Engineering A, **374**, 327 (2004).
- [2] B.G.Choi, I.S.Kim, D.H.Kim, C.Jo; Materials Science and Engineering A, **478**, 329 (2008).
- [3] S.A.Sajjadi, S.Nategh, R.I.L.Guthrie; Materials Science and Engineering A, **325**, 484 (2002).
- [4] C.T.Liua, J.Ma, X.F.Sun; Journal of Alloys and Compounds, **491**, 522 (2010).
- [5] S.A.Sajjadi, S.Nategh; Materials Science and Engineering A, **307**, 158 (2001).
- [6] F.Long, Y.S.Yoo, C.Y.Jo, S.M.Seo, Y.S.Song, T.Jin, Z.Q.Hu; Materials Science and Engineering A, **527**, 361 (2009).

- [7] S.A.Sajjadi, S.M.Zebarjad, R.I.L.Guthrie, M.Isac; *Materials Processing Technology*, **175**, 376 (2006).
- [8] M.Pouranvari, A.Ekrami, A.H.Kokabi; *Alloys and Compounds*, **461**, 641 (2008).
- [9] A.Jacques, F.Diologent, P.Caron, P.Bastie; *Materials Science and Engineering A*, **483-484**, 568 (2008).
- [10] A.D.Sequeira, H.A.Calderon, G.Kostorz; *Scripta Metallurgica Materialia*, **30**, 75 (1994).
- [11] T.Grosdidier, A.Hazotte, A.Simon; *Scripta Metallurgica Materialia*, **30**, 1257 (1994).
- [12] S.Kraft, I.Altenberger, H.Mughrabi; *Scripta Metallurgica Materialia*, **32**, 411 (1995).
- [13] Y.Y.Qiu; *Acta Materialia*, **44**, 4969 (1996).
- [14] S.H.Mousavi Anijdan, A.Bahrami; *Materials Science and Engineering A*, **396**, 138 (2005).
- [15] G.E.Fuchs; *Mater.Sci.Eng.A*, **300**, 52 (2001).
- [16] G.E.Fuchs; *J.Mater.Eng.Perform.*, **11**, 1925 (2002).
- [17] N.El-Bagoury, A.Nofal; *Journal of Materials Science and Engineering A*, **527**, 7793 (2010).
- [18] M.T.Kim, S.Y.Chang, J.B.Won; *Material Science and Engineering A*, **441**, 126 (2006).
- [19] N.El-Bagoury, M.A.Waly, A.A.Nofal; *Materials Science and Engineering A*, **487**, 152 (2008).
- [20] J.X.Yang, Q.Zheng, X.F.Sun, H.R.Guan, Z.Q.Hu; *Scripta Materialia*, **55**, 331 (2006).
- [21] Nader El-Bagoury, Q.Mohsen; 'TCP and Gamma Prime Phases and Mechanical Properties of Thermally Exposed Ni Base Superalloy' under Publications.
- [22] Nader El-Bagoury; 'New Gamma Phase Formation Mechanism during Solution Treatment of an Experimental Ni base Superalloys' under Publication.
- [23] X.Z.Qin, J.T.Guo, C.Yuan, G.X.Yang, L.Z.Zhou, H.Q.Ye; *Journal of Materials Science*, **44**, 4840 (2009).